

Rapid Commun. Mass Spectrom. 2013, 27, 1505–1516
(wileyonlinelibrary.com) DOI: 10.1002/rcm.6598

Ultraviolet degradation of procymidone – structural characterization by gas chromatography coupled with mass spectrometry and potential toxicity of photoproducts using *in silico* tests

Ahmad Rifai^{1,2}, Yasmine Souissi¹, Christophe Genty¹, Carine Clavaguera¹,
Sophie Bourcier¹, Farouk Jaber² and Stéphane Bouchonnet^{1*}

¹Laboratoire des Mécanismes Réactionnels UMR-7651, Ecole Polytechnique, 91128 Palaiseau Cedex, France

²Laboratoire d'Analyse des Pesticides et des Polluants Organiques - Commission Libanaise de l'Énergie Atomique - Centre National de Recherches Scientifiques - Beyrouth, Liban

RATIONALE: Procymidone is a dicarboximide fungicide mainly used for vineyard protection but also for different crops. The structural elucidation of by-products arising from the UV-visible photodegradation of procymidone has been investigated by gas chromatography coupled with mass spectrometry. The potential toxicities of photoproducts were estimated by *in silico* tests.

METHODS: Aqueous solutions of procymidone were irradiated for up to 90 min in a self-made reactor equipped with a mercury lamp. Analyses were carried out on a gas chromatograph coupled with an ion trap mass spectrometer operated in electron ionization and methanol positive chemical ionization. Multistage collision-induced dissociation (CID) experiments were performed to establish dissociation pathways of ions. Toxicities of byproducts were estimated using the QSAR T.E.S.T. program.

RESULTS: Sixteen photoproducts were investigated. Chemical structures were proposed mainly based on the interpretation of multistage CID experiments, but also on their relative retention times and kinetics data. These structures enabled photodegradation pathways to be suggested. Only three photoproducts remain present after 90 min of irradiation. Among them, 3,5-dichloroaniline presents a predicted rat LD50 toxicity about ten times greater than that of procymidone.

CONCLUSIONS: 3,5-Dichloroaniline is the only photoproduct reported in previous articles. Eight by-products among the sixteen characterized might be as toxic, if not more, than procymidone itself considering the QSAR-predicted rat LD50. Copyright © 2013 John Wiley & Sons, Ltd.

Procymidone is a dicarboximide fungicide mainly used for vineyard protection but also for strawberry, flowers and various ornamental cultivations.^[1,2] According to the European Commission directive 2006/132/EC, all Member States of the European Union (EU) should amend or withdraw existing authorizations for plant protection products containing procymidone as an active substance. In 2010, the EU set the Maximum Residue Level (MRL) of procymidone in crops at 0.02 mg/kg.^[3] Procymidone presents anti-androgen toxicity and ability to induce developmental and/or reproductive dysfunctions by interfering with the endocrine system of exposed organisms^[4–7] and is a member of the endocrine disruptor family.^[8] The United States Environmental Protection Agency reported that procymidone and its main metabolite, 3,5-dichloroaniline (3,5-DCA), are

carcinogenic products with dietary assessment.^[9] Thus, the detection of this pesticide and its metabolites in environmental samples is a priority in quality control. The transformation of pesticides in the environment is a highly complex process affected by many physical and chemical factors.^[10] According to Burrows *et al.*, most pesticides are resistant to chemical and/or photochemical degradation under typical environmental conditions and very little information is available regarding their natural degradation processes, the quality, structure and biological impact of their degradation products.^[11] Previous studies devoted to the degradation of procymidone have been focused on photocatalytic degradation techniques. Hustert and Moza studied the photochemical degradation of procymidone and vinclozolin in water using a mercury lamp with $\lambda \geq 290$ nm. This study established that the addition of Fe₂O₃ and TiO₂ catalyzes the photodegradation of both compounds and that the presence of humic and fulvic acids (naturally extracted by the water from the soil constituents) increases the rate of photodegradation. Monodechlorination, didechlorination and isomerization are the major photo degradation pathways.^[12] Schwack

* Correspondence to: S. Bouchonnet, Laboratoire des Mécanismes Réactionnels UMR-7651, Ecole Polytechnique, 91128 Palaiseau Cedex, France.
E-mail: stephane.bouchonnet@polytechnique.edu

et al. studied the potential of procymidone to undergo photo-induced processes in the presence of different organic groups. Their objectives were to find an explanation for the formation of bound residues in plant cuticles in the presence of polymer molecules, waxes and cutin. In isopropanol, cyclohexane and cyclohexene, photodegradation led to substitution of a chlorine atom by a solvent molecule.^[13] Vanni and co-workers studied the degradation of procymidone in agricultural land under various pH and temperature conditions. They reported that the total degradation of procymidone occurred at alkaline pH and at high temperature in a few days; the main metabolite detected in their studies was 3,5-DCA.^[14] The present study aims to identify photodegradation products of procymidone in water and to assess their potential toxicity. It is now well admitted that sunlight absorbance in water may be significantly modified by the presence of dissolved organic matter but we consider here that photodegradation may start as soon as the aqueous solution of herbicide is sprayed on leaves and fruits, under intense sunlight irradiation. This study was first devoted to the structural elucidation of photoproducts using multiple-stage mass spectrometry coupled with gas chromatography (GC/MSⁿ). Structural elucidation of photoproducts was performed on the basis of the collision-induced dissociations observed in both electron ionization and positive chemical ionization modes. Photolysis mechanisms were also suggested to explain the formation of the photoproducts formed from irradiated procymidone in water. An approach of quantitative structure–activity relationship (QSAR) was used to assess the potential toxicity effect of procymidone and of its photodegradation products. For that purpose we used a Toxicity Estimation Software Tool (T.E.S.T.), a U.S. Environmental Protection Agency developed program, to predict mutagenicity, oral rat lethal doses, developmental toxicity as well as growth inhibition concentrations and lethal doses of aquatic organisms.

EXPERIMENTAL

Chemicals and reagents

Procymidone (99% purity) was purchased from Sigma Aldrich (St Quentin Fallavier, France). The chemical structure of procymidone is shown in Fig. 1. Chromatographic grade solvents (99.99% purity), methylene chloride and acetonitrile (ACN), were also purchased from Sigma Aldrich. Considering the poor solubility of procymidone in water (4.5 mg/L at 25 °C), a solution of procymidone at 100 mg/L

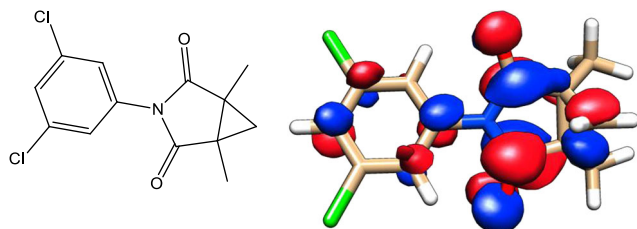


Figure 1. Chemical structure of procymidone and nature of the first excited state (CC2 level).

was first prepared in ACN. This solution was then used to prepare working solutions in water at 5.0 mg/L. This high concentration was used for structural investigations on photoproducts as multi-stage mass spectrometry experiments require relatively high analyte concentrations. Aqueous solutions at 0.5 mg/L were used for kinetic measurements.

Photolysis experiments

Photolysis experiments were carried out in a self-made reactor equipped with a high-pressure mercury lamp (HPL-N 125 W/542 E27 SC; Phillips, Ivry-sur-Seine, France) delivering radiation at wavelengths ranging from 200 to 650 nm. The absorbance spectrum of procymidone displays an absorption maximum between 200 and 208 nm.^[15] According to the manufacturer's data, the incident radiation flux was 6200 lm. The reactor consists of six quartz tubes of 120 mL arranged in a circle around the lamp and immersed into a sonicator (AL04-12, Advantage-Lab, Switzerland) filled with deionized water. During experiments, the reactor was regularly cooled by addition of ice to avoid uncontrolled heating of the irradiated solutions and to maintain a constant temperature of 25 ± 3 °C. For each experiment, 50 mL of a solution of procymidone (see above) were used.

Sample preparation

After photolysis, 6 mL of solution were taken from the quartz tube and transferred into a separating funnel. Methylene chloride (6 mL) was added to the solution which was then shaken and left to settle for 10 min. The organic phase was collected and dried under a gentle nitrogen stream and the dry residue was dissolved into 200 µL of methylene chloride for GC/MS analysis.

GC and MS operating conditions

Analyses were carried out on a Varian 450GC gas chromatograph equipped with a CP8400 autosampler and coupled with a VARIAN 240MS ion trap mass spectrometer operated in the internal ionization mode. A 60-m-long 'VF-Xms' capillary column (VARIAN) with an i.d. of 0.25 mm and a film thickness of 0.25 µm was used. For all analysis, 2 µL of solution were injected automatically in the splitless mode at a rate of 50 µL s⁻¹. The injector temperature was set to 280 °C and high-purity helium (99.999 %) was used as carrier gas at a constant flow of 1.4 mL min⁻¹. The column oven temperature was programmed from an initial temperature of 50 °C held during 1 min, increased to 280 °C at 15 °C/min, held for 5 min at 280 °C, then increased at 10 °C/min to a final temperature of 300 °C, which was held for 20 min, for a total analysis duration of 43 min. The manifold, the ion-trap electrodes and the transfer line temperatures were respectively held at 100, 200 and 280 °C. The mass spectrometer was calibrated with the ions resulting from electron ionization (EI) of perfluorotributylamine. Chemical ionization (CI) experiments were performed using methanol as the reagent. Spectra were recorded using the automatic gain control (AGC) function with target values fixed at 20 000 and 5000 for EI and CI, respectively. The filament emission current was set at 10 µA in EI and 50 µA in CI. The electron multiplier voltage was automatically optimized at 2200 V for a gain value of 10⁵. Full

scan mass spectra were acquired recording ions from m/z 50 to 500 at a scan rate of 0.33 s/scan, each spectrum resulting from ion acquisitions on 5 microscans. In multi-stage mass spectrometry (MS^n) experiments, precursor ions were stored with a Paul stability parameter (qz) of 0.30 and fragmented by collision-induced dissociation (CID) with activation energies ranging from 0.30 to 0.80 V in the resonant excitation mode.

Quantum chemistry calculations

Geometry optimizations were performed at the DFT/B3LYP-D3 level, including the new implementation of dispersion corrections^[16,17] in the TURBOMOLE 6.4 package.^[18] The minima were characterized by vibrational frequency calculations. All the calculations were carried out with the polarized valence-triple-zeta TZVPP basis set. The most energetically stable geometry of the molecule (Fig. 1) was used for the calculation of the electronic excited states by both the CC2 coupled cluster model and the time-dependent density functional theory (TD-DFT) using the B3LYP-D3 functional. The CC2 equations are an approximation to the coupled cluster singles and doubles (CCSD) ones.^[19] This method is considered as an accurate tool for the investigation of the excited states of molecules.^[20] Regarding the nature and the transition energies, both methods provide similar results that will be described in the Results section (see Supplementary Table S1, Supporting Information).

Computer-aided toxicity prediction

The Toxicity Estimation Software Tool (T.E.S.T.) is an Environmental Protection Agency online available computerized predictive system with Quantitative Structure Activity Relationships (QSAR) mathematical models.^[21] T.E.S.T. has a variety of toxicity endpoints used to predict chemical toxicity values from their physical properties such as molecular structure. The T.E.S.T. model uses a simple linear function of molecular descriptors such as the octanol-water partition coefficient, molecular weight or the number of benzene rings (see Eqn. (1)):

$$\text{Toxicity} = ax_1 + bx_2 + c \quad (1)$$

where x_1 and x_2 are independent descriptor variables and a , b , and c are fitted parameters. Models for assessing toxicity solely from molecular structure are based on information-rich structural descriptors that quantify transport, bulk, and electronic attributes of a chemical structure. Besides molecular weight, the QSAR model employs size-corrected E-values for quantification of molecular bulk. The size-corrected E-values are computed from a rescaled count of valence electrons.^[22] Electrotopological state values (E-values), as numerical quantifiers of molecular structure, encode information about the electron content (valence, sigma, pi and lone-pair), topology, and environment of an atom, or a group of atoms, in a molecule.^[22] The predicted toxicity is estimated by taking an average of the predicted toxicities from the above QSAR methods, provided the predictions are within the respective applicability domains.

RESULTS AND DISCUSSION

Characterization of the photoproducts of procymidone

A series of experiments was performed with eight irradiation times ranging from 0 to 90 min: 0, 5, 10, 15, 20, 40, 60 and 90 min. The comparison of the corresponding chromatograms, recorded in the EI mode, showed that the relative abundances of photoproducts vary significantly according to the irradiation time. The relative abundances of photoproducts are plotted as a function of the irradiation time in Fig. 2. A precise quantitation of photoproducts was not possible given the lack of standards. Thus abundances were just estimated by integrating chromatographic peaks on the total ion current (TIC); they are expressed in Fig. 2 in an arbitrary unit proportional to the TIC. The abundance of procymidone was not plotted because it was out of scale. Disappearance of procymidone follows a pseudo-exponential type curve. Only 5% of the initial amount of procymidone is still detected after 60 min of irradiation. Procymidone is no longer detected after 90 min of irradiation. Among the 16 photoproducts detected, 13 are formed as soon as irradiation begins; their concentrations reach maximum values for photolysis times around 10 min before decreasing to reach trace amounts after 40 min of irradiation. The three other compounds, referred as 1, 2 and 7 (see numbering in Table 1), are also detected as soon as irradiation begins; their concentrations rapidly increase during the first 30 min and go on increasing at a

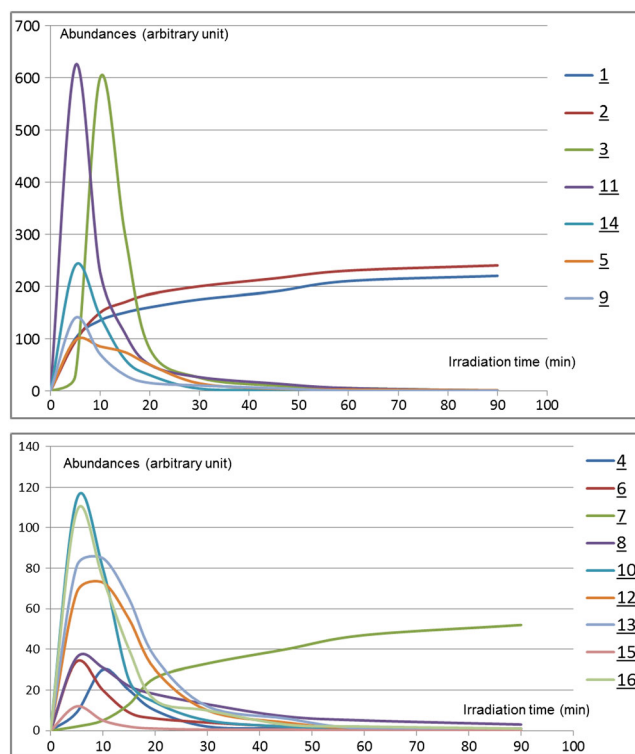
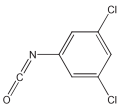
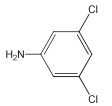
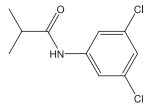
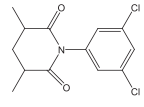
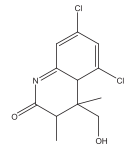
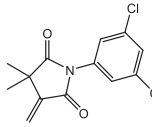
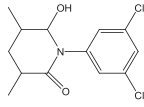
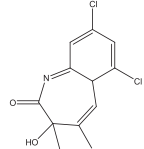
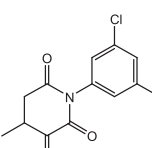


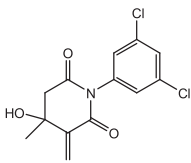
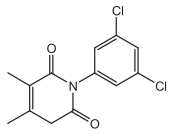
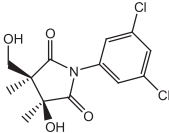
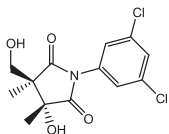
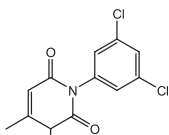
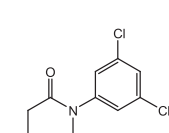
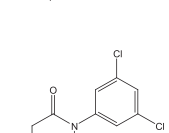
Figure 2. Abundances of photoproducts (arbitrary unit) as a function of the irradiation time (refer to Table 1 for the numbering of compounds). Abundances of major compounds (1, 2, 3, 5, 9, 11 and 14) are plotted at the top of the figure; abundances of minor compounds (4, 6, 7, 8, 10, 12, 13, 15 and 16) are plotted at the bottom of the figure.

Table 1. Molecular weights measured, retention times, relative abundances after 15 min of irradiation and main MSⁿ transitions recorded in GC/MS with both CI and EI ionization modes for photolysis products of procymidone. Suggested structures based on mass spectra interpretation are given in the right-hand column

	Molecular weight measured	Retention time (min)	Relative abundance ^a	Main transitions in CI-MS ⁿ (<i>m/z</i>)	Main transitions in EI-MS ⁿ (<i>m/z</i>)	Chemical structure proposed
<u>1</u>	187	17.00	11.5	188 → 160 (-28) 188 → 153 (-35) 153 → 125 (-28) 125 → 90 (-35)	187 → 159 (-28) 159 → 124 (-35) 124 → 97 (-27)	
<u>2</u>	161	20.27	10.3	162 → 127 (-35) 127 → 126 (-1) 126 → 100 (-26)	161 → 134 (-27) 134 → 99 (-35) 161 → 126 (-35)	
<u>3</u>	231	25.45	12.6	232 → 162 (-70) 162 → 127 (-35)	231 → 187 (-44) 187 → 152 (-35) 231 → 161 (-70) 161 → 126 (-35)	
<u>4</u>	285	28.80	1.7	286 → 258 (-28) 258 → 230 (-28) 230 → 202 (-28)	285 → 257 (-28) 257 → 187 (-70) 187 → 152 (-35) 187 → 145 (-42) 145 → 110 (-35)	
<u>5</u>	273	29.71	5.9	274 → 256 (-18) 256 → 228 (-28) 274 → 246 (-28) 246 → 218 (-28)	273 → 245 (-28) 245 → 161 (-84) 161 → 126 (-35)	
<u>6</u>	283	30.26	2.3	284 → 186 (-98) 284 → 256 (-28) 256 → 238 (-18) 238 → 221 (-28) 221 → 181 (-40) 181 → 165 (-18)	283 → 255 (-28) 255 → 254 (-1) 254 → 226 (-28) 226 → 191 (-35)	
<u>7</u>	287	30.42	1.4	288 → 270 (-18) 270 → 242 (-28) 242 → 240 (-2)	287 → 259 (-28) 259 → 189 (-70) 189 → 161 (-28) 161 → 126 (-35)	
<u>8</u>	271	30.54	1.9	272 → 256 (-16) 272 → 244 (-28)	271 → 256 (-15) 256 → 228 (-28) 228 → 200 (-28) 200 → 265 (-35)	
<u>9</u>	283	30.99	5.6	284 → 256 (-28) 256 → 241 (-15) 241 → 203 (-38) 203 → 185 (-18) 203 → 158 (-45) 158 → 130 (-28)	283 → 268 (-15) 268 → 240 (-28) 240 → 205 (-35) 283 → 241 (-42) 241 → 213 (-28) 213 → 178 (-35)	

(Continues)

Table 1. (Continued)

	Molecular weight measured	Retention time (min)	Relative abundance ^a	Main transitions in CI-MS ⁿ (<i>m/z</i>)	Main transitions in EI-MS ⁿ (<i>m/z</i>)	Chemical structure proposed
<u>10</u>	299	31.39	5.5	300 → 258 (-42) 258 → 240 (-18) 258 → 230 (-28) 230 → 186 (-44)	299 → 282 (-17) 299 → 257 (-42) 257 → 256 (-1) 256 → 221 (-35)	
<u>11</u>	283	31.57	15.3	284 → 256 (-28) 256 → 238 (-18) 228 → 193 (-35) 193 → 178 (-15) 193 → 158 (-35)	283 → 268 (-15) 268 → 240 (-28) 240 → 205 (-35)	
<u>12</u>	315	31.73	5.3	316 → 298 (-18) 298 → 270 (-28) 270 → 242 (-28)	315 → 300 (-15) 300 → 272 (-28) 272 → 244 (-28) 315 → 298 (-17) 298 → 270 (-28) 270 → 242 (-28)	
<u>13</u>	315	31.77	5.3	316 → 298 (-18) 298 → 270 (-28) 270 → 242 (-28)	315 → 300 (-15) 300 → 272 (-28) 272 → 244 (-28) 315 → 298 (-17) 298 → 270 (-28) 270 → 242 (-28)	
<u>14</u>	283	31.97	9.7	284 → 256 (-28) 256 → 238 (-18) 238 → 203 (-35) 203 → 167 (-36)	283 → 268 (-15) 268 → 240 (-28) 240 → 205 (-35) 283 → 256 (-27) 256 → 228 (-28) 228 → 193 (-35)	
<u>15</u>	283	32.46	0.5	284 → 256 (-28) 256 → 238 (-18) 238 → 223 (-15) 238 → 200 (-38) 200 → 169 (-31) 200 → 154 (-46)	283 → 256 (-27) 256 → 228 (-28) 228 → 193 (-35)	
<u>16</u>	281	33.90	5.2	282 → 264 (-18) 264 → 229 (-35)	281 → 253 (-28) 253 → 252 (-1) 252 → 217 (-35) 281 → 229 (-52) 229 → 201 (-28) 201 → 200 (-1) 200 → 165 (-35)	

^a% of the total of all the product abundances.

slower rate until the end of the experiment; 1, 2 and 7 are the only by-products remaining in significant amounts in water after 90 min of irradiation of procymidone.

All degradation products were detected with a significant abundance ($\geq 2\%$) in the solution corresponding to an irradiation time of 15 min. This solution was then chosen to

perform MSⁿ experiments on all the photoproducts. The corresponding chromatogram is displayed in Fig. 3. Peaks that are not numbered correspond to compounds that are detected in the non-irradiated reference solution of procymidone (corresponding to $t=0$), which has undergone the same sample preparation process. Only the compounds

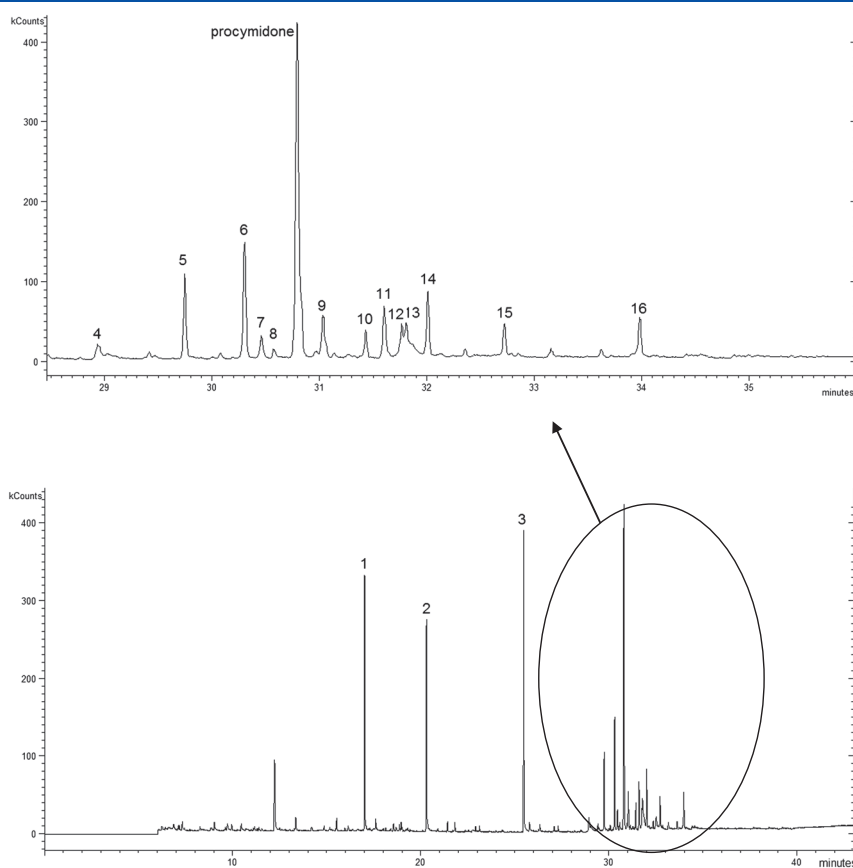


Figure 3. Chromatogram (EI mode) of an aqueous solution of procymidone at 5 mg/L irradiated for 15 min. Non-numbered peaks correspond to compounds also detected in the non-irradiated solution.

detected with a signal-to-noise ratio higher than 10 were investigated. A few articles report the analysis of procymidone using LC/MS coupling with an ESI source in positive mode.^[14,23,24] We did not succeed in detecting procymidone in LC/MS whatever the device used: HPLC/Q-TOF and nanoLC/FT-ICR. Nevertheless, the comparison of the total ion currents of the photoproducts in the chromatograms of the irradiated solutions with that of procymidone in the reference solution suggests that more than 90% of products are detected by GC/MS.

Nominal molecular weights of the photoproducts of procymidone were easily determined. For each compound, the heavier ion (often also the most abundant one) in the CI mass spectrum was first assumed to correspond to the MH^+ pseudo-molecular ion. This assumption was systematically confirmed by the presence of an ion at $m/z = M$ (assumed to correspond to M^+) in significant abundance in the EI spectrum. Molecular weights are reported in Table 1.

According to literature data devoted to the photolysis of chlorinated compounds, the loss of the chlorine atom under irradiation often constitutes the first step of the degradation process.^[25–27] In the case of procymidone, the isotopic distributions observed for M^+ and MH^+ ions of photoproducts show that chlorine atoms were not removed by photolysis in any case.

Compounds **1** and **2** were identified as 1,3-dichloro-5-isocyanatobenzene and 3,5-dichlorobenzamine, respectively, with probabilities greater than 95% according

to the NIST spectral database so that no particular structural investigation was carried out.^[28] Compounds **6**, **9**, **11**, **14** and **15** have the same nominal molecular weight ($MW = 283$ amu for the major isotopomer including two ^{35}Cl atoms) as procymidone and were assumed to be isomers of the latter. A mechanism has been suggested (see Fig. 4) to rationalize isomerization of procymidone under irradiation. The TD-DFT and CC2 calculations reveal that the first excited state of procymidone corresponds to a triplet spin state with an excitation from the dichlorophenyl group to the two $\text{C}=\text{O}$ groups (Fig. 1). Consequently, it can be considered that the oxygen atoms constitute the most favorable ionization sites of procymidone. In the gas phase, electron ionization of a carbonyl function is followed by the heterolytic cleavage of the bond(s) in alpha; this is referred as alpha cleavage by mass spectrometrists.^[29] We postulated that the same alpha cleavage occurs in aqueous solution and is accompanied by the aperture of the strained three-centered ring. This leads to a distonic ion displayed in the form of three mesomeric structures referred as a, b and c at the left-hand side of Fig. 4. Like in mass spectrometry, we considered that the reactivity induced by the radical should be greater than that induced by the charge, the latter being furthermore stabilized by surrounding water molecules in the present experiment. In aqueous solution, the radical can react with a water molecule to abstract a hydrogen atom or a hydroxyl

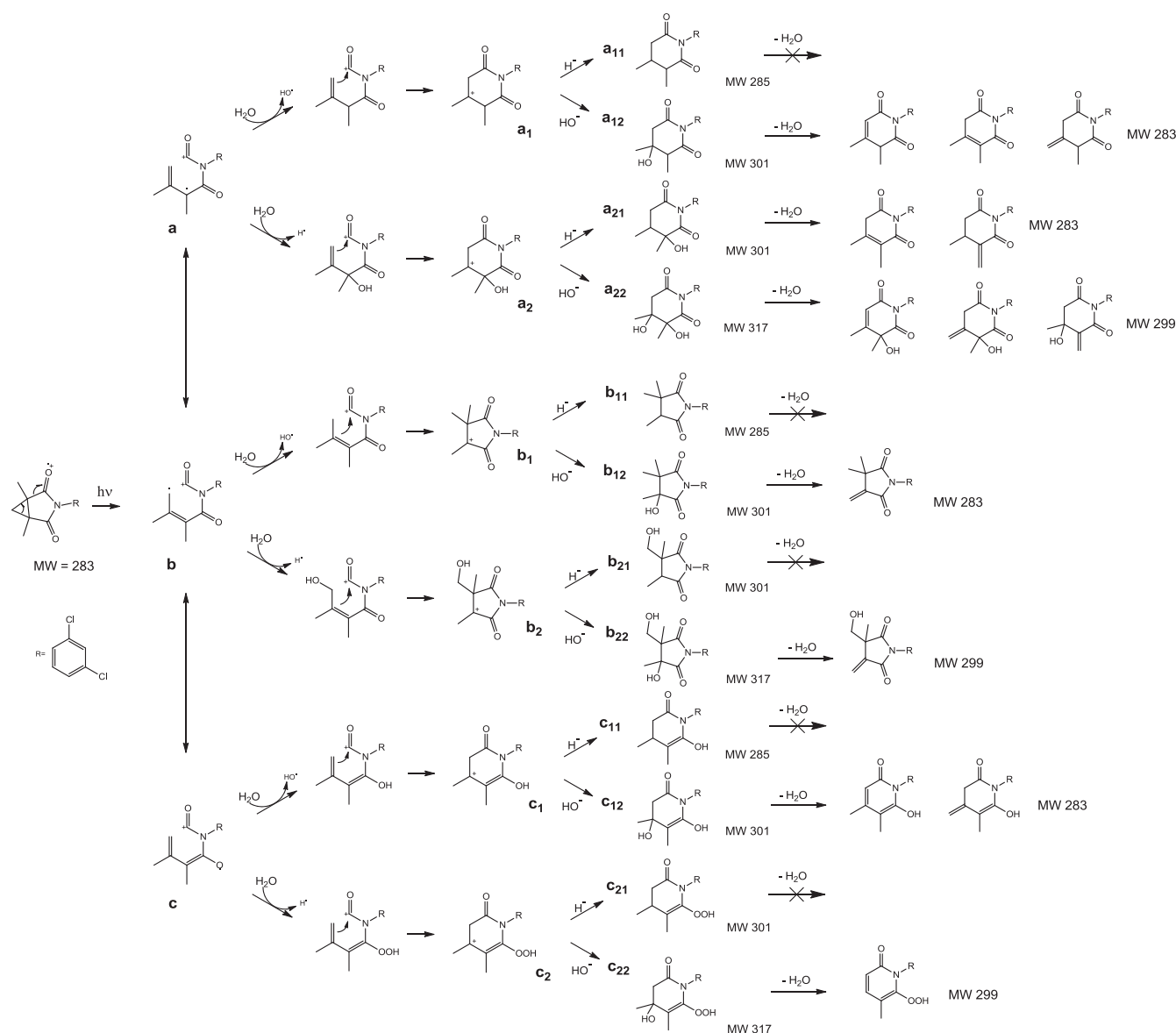


Figure 4. Mechanisms proposed to explain the isomerization of procymidone under irradiation in water.

radical. Both cases were considered from each mesomeric form to provide six structures that may likely cyclize to lead to carbocations better stabilized by inductive and mesomeric effects. The cyclized structures are referred as a_1, a_2, b_1, b_2, c_1 and c_2 in Fig. 4. In pure water, those six even-numbered electron cations may each react with a water molecule by capturing either a hydride H^- or a hydroxyl anion OH^- . Considering both hypotheses leads to the twelve structures displayed at the right-hand side of Fig. 4. a_{11} and a_{12} result respectively from capture by a_1 of H^- and of OH^- . The same notation is used for structures b_{11}, b_{12}, c_{11} , etc.

They are six photoproducts detected with the same nominal molecular weight (283 amu) as procymidone and with close retention times (ranging from 30.26 to 32.46 min) around that of procymidone (30.8 min). Figure 4 shows that six compounds with the same nominal mass (283) as

procymidone (and thus assumed to be isomers of the latter) can be formed according to the mechanisms suggested: water loss from a_{12} leads to three isomers, water loss from a_{21} provides two isomers (one of which is common with one issued from a_{12}), water loss from b_{12} gives the only five-membered ring isomer and water loss from c_{12} leads to two tautomeric forms of isomers issued from a_{12} . Compounds 6, 9, 11, 14 and 15 were assumed to correspond to these five isomers. Their chemical structures were elucidated on the basis of the MS^n experiments performed in the EI mode. For the molecular ion of each structure, the charge has been assumed to be carried by one of the oxygen atoms according to the results of quantum chemistry calculations (see above). As shown in Fig. 5, alpha cleavage leads to distonic ions whose reactivity is largely driven by the radical. 6 is the only structure for which the alpha cleavage from M^+ leads to a tertiary radical stable enough to permit monoxide elimination

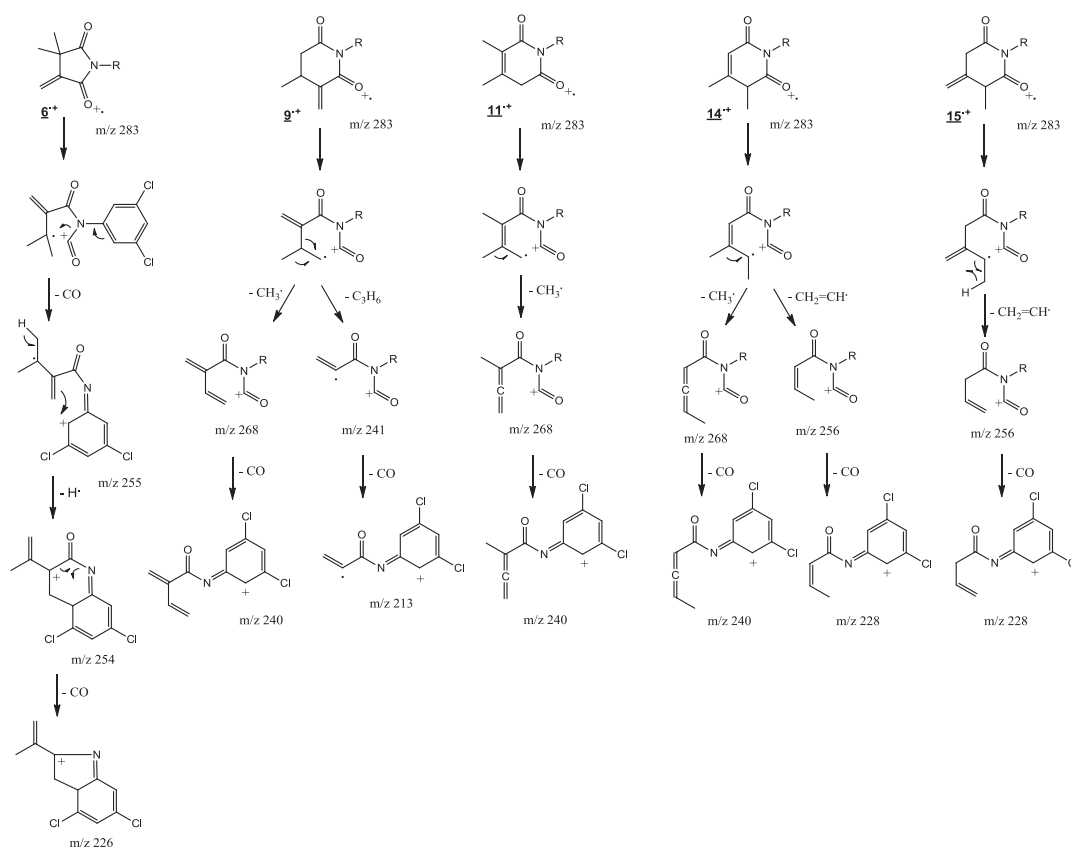


Figure 5. Dissociation pathways in EI-MSⁿ of compounds 6, 9, 11, 14 and 15.

prior to radical elimination. 9 corresponds to the only structure that can eliminate CH₃ and CH₂=CH-CH₃ following electron ionization (transitions m/z 283 → 268 and m/z 283 → 241 in Table 1). 11 corresponds to the structure that can only eliminate CH₃ from M⁺ (transition m/z 283 → m/z 268 in Table 1). 14 corresponds to the structure that can eliminate CH₃ and CH₂=CH from M⁺ (transitions m/z 283 → 268 and m/z 283 → 256 in Table 1). Finally, 15 corresponds to the structure that can only eliminate CH₂=CH from M⁺ (transition m/z 283 → 256 in Table 1). It is to be noted that Cl losses are not displayed in Fig. 4 because they result from homolytic cleavages under high activation energies that do not contribute to distinguish isomers in the present case.

Compound 4 (285 amu, see Table 1) could correspond to one of the structures a₁₁, b₁₁ or c₁₁, the latest corresponding to the enolic form of a₁₁, in Fig. 4. The fact that only one isomer is detected rather suggests the symmetrical structure displayed in Table 1 whose formation is easily explained by consecutive captures of a hydrogen atom and a hydride ion by ionized procymidone, according to the mechanism detailed in Fig. 6. This hypothesis is supported by the fact that the symmetrical structure proposed for 4 is the only one allowing the transitions observed in CI-MSⁿ (m/z 286 → 258 230 → 202); the corresponding mechanisms are given in Supplementary Fig. S1 (see Supporting Information). These three consecutive losses of 28 amu in CI-MSⁿ are not possible from a₁₁, b₁₁ nor c₁₁. The formation of compound 7 (287 amu, see Table 1) can be rationalized by consecutive additions of a hydrogen atom and a hydride ion on 4 after ionization of the

latter, by a mechanism analogous to that proposed for the formation of 4 from ionized procymidone (Fig. 5). EI-MSⁿ and CI-MSⁿ transitions recorded for 7 are rationalized in Supplementary Fig. S2 (see Supporting Information). Concerning compound 3 (MW 231, eluted at 25.45 min), the losses of 70 amu in CI-MS² and 44 amu in EI-MS² suggest that a C₃H₇CO group is bound to the nitrogen atom. The chemical structure including an isopropyl group displayed in Table 1 for 3 may be formed after photoionization of 4, as proposed in Fig. 6. Kinetics data show that the formation of 7 and 3 is accompanied by the disappearance of 4 (see above); this strongly supports the hypothesis according to which 3 and 7 would result from photoionization of 4. EI-MSⁿ and CI-MSⁿ transitions recorded for 3 are rationalized in Supplementary Fig. S2 (see Supporting Information). The dissociation pathways of 3 in EI-MSⁿ lead to ions at m/z 187 and 161 which correspond respectively to the ionized compounds 2 and 1.

Compound 5 has a molecular weight of 273 amu; its formation likely results from HO addition on ionized procymidone followed by CO elimination and hydride addition, as displayed in Fig. 7. Figure 6 shows that three isomers with molecular weight of 273 amu can be formed from structures a, b and c (see Fig. 4) according to such a mechanism. The consecutive transitions m/z 273 → 245 → 161 in CI-MS³ suggest that the detected isomer is that issued from structure b in Fig. 7, based on the dissociation pathways proposed in Supplementary Fig. S3 (see Supporting Information). Compound 8 has a molecular weight of

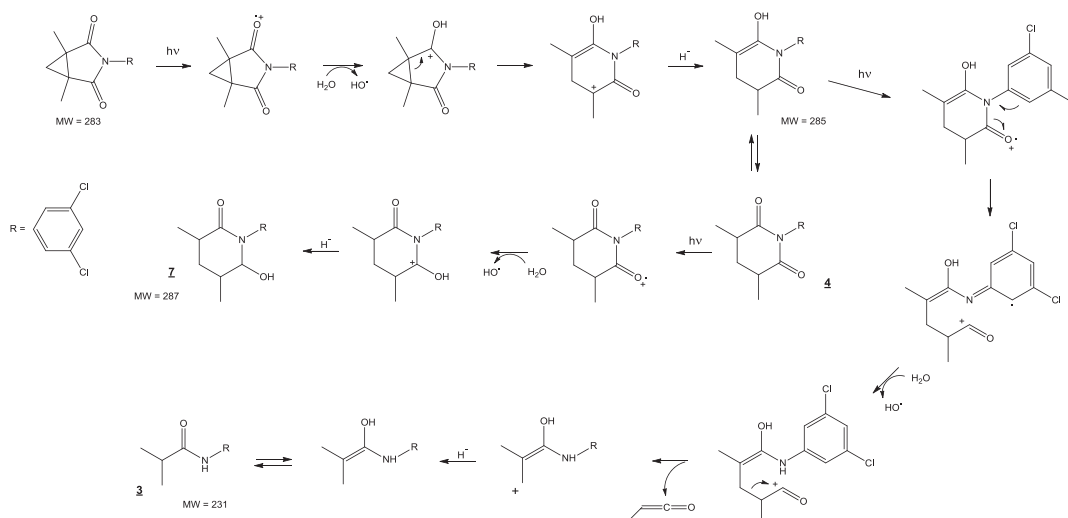


Figure 6. Mechanisms proposed to explain the formation of compounds 3, 4 and 7 from irradiated procymidone in water.

271 amu; its formation likely results from HO[•] addition on ionized procymidone followed by CO elimination and proton elimination, as displayed in Fig. 7. Five isomers with a nominal mass of 271 can be formed from structures a, b and c according to such a mechanism. The only isomer allowing consecutive losses of a methyl radical and two carbon monoxide molecules in EI-MSⁿ (m/z 271 → 256 → 228 → 200) is one of those issued from structure a in Fig. 7 (see Table 1). Dissociation pathways suggested to explain the recorded EI-MSⁿ and CI-MSⁿ transitions for 8 are given in Supplementary Fig. S4 (see Supporting Information).

Compound 10 (MW 299 amu) was detected at 31.39 min. Based on the reactions in Fig. 4, five isomers with molecular weight of 299 amu can be easily formed from photo-ionized procymidone. The CI-MSⁿ transitions, especially m/z 300 → 258 and m/z 258 → 240 (consecutive losses of CH₂=CO and H₂O) allowed a conclusion in favor of the structure proposed in Table 1 (one of the structures issued from a₂₂ in Fig. 4), according to the dissociation pathways provided in Supplementary Fig. S5 (see Supporting Information). Compounds 12 and 13 have the same molecular weight of 315 amu, which, compared with the MW of procymidone (283 amu), may likely correspond to the addition of two hydroxyl groups and the loss of H₂. Figure 4 displays three isomers with MW 317 amu resulting from the addition of two hydroxyl groups on procymidone: a₂₂, b₂₂ and c₂₂. Among them, only b₂₂ can easily eliminate H₂ through oxidation of an alcohol function into an aldehyde one. Compounds 12 and 13 provide exactly the same transitions in EI-MSⁿ and CI-MSⁿ experiments (see Table 1) and have very close retention times (31.73 and 31.77 min, respectively). This led us to consider 12 and 13 as two diastereoisomers of b₂₂ (see Fig. 4) whose formation under irradiation would be explained by the mechanism suggested in Fig. 8. The fact that both compounds are formed in equal ratios is in good agreement with this mechanism. The EI-MSⁿ and CI-MSⁿ transitions perfectly match the structures proposed in Table 1 for 12 and 13; the corresponding dissociation pathways are displayed in Supplementary Fig. S6 (see Supporting Information). Compound 16 (281 amu) was assumed to result from

dehydrogenation of procymidone. A mechanism involving consecutive losses of H[•] and H⁺ from ionized procymidone has been proposed in Fig. 8. Mechanisms corresponding to the EI-MSⁿ and CI-MSⁿ transitions observed for 16 are proposed in Supplementary Fig. S7 (see Supporting Information).

Toxicity prediction

In order to evaluate the toxicity of procymidone and its photodegradation products, a toxicity simulation using *in silico* tools was performed. We chose in this study only to report the significant results, i.e. oral rat LD₅₀ toxicity (Fig. 9).

We observed that the procymidone and all its identified photodegradation products exhibit a developmental toxicity. Procymidone was reported in the literature as being a competitive antagonist to the androgen binding to their receptor causing thereby development in male offspring.^[30] The effects on reproduction and the induction of testicular tumors in a long-term rat study can be explained by the effects of procymidone on the endocrine system.^[31] A recent study stated that this dicarboximide fungicide reduces weights of the prostate and seminal vesicle.^[32] Thus the procymidone developmental toxicity prediction through the QSAR simulation was coherent with the literature data. It is to be noticed that all degradation products generated through procymidone photolysis kept the 3,5-dichloroaniline (3,5-DCA) on the molecule skeleton. The U. S. Environmental Protection Agency treats 3,5-DCA as a cancer-causing chemical based on the carcinogenicity of the structurally related compound *p*-chloroaniline.^[33] This metabolite was reported as the final product of the degradation metabolic pathway of dicarboximide fungicides.^[14] It also was assigned as more toxic and persistent than one of its parent compounds: vinclozolin. In particular, toxicity of 3,5-DCA has been shown to be related to anti-androgenic activity.^[34] The hypothesis of developmental toxicity potential related to the 3,5-DCA common part of all degradation products is then postulated.

Procymidone is of low acute toxicity by the oral route. Its rat and mice oral LD₅₀ was reported in the literature to be >5000 mg/kg.^[31] The displayed value of oral rat LD₅₀ by

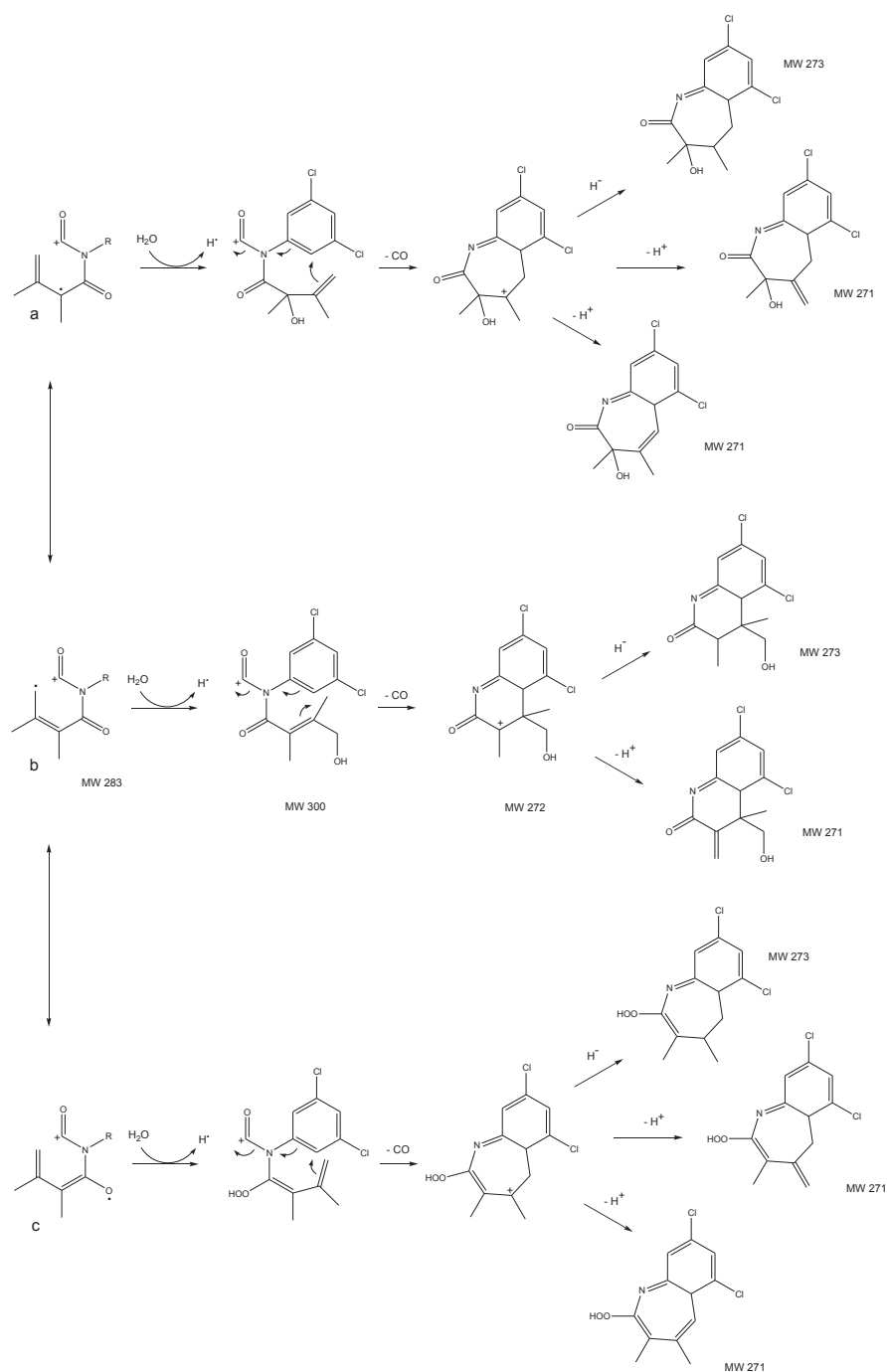


Figure 7. Mechanisms proposed for the formation of compounds with molecular weights of 271 and 273 amu from irradiated procymidone in water (structures a, b and c are mesomeric forms resulting from the aperture of the five-membered ring of ionized procymidone, see Fig. 3).

the simulation software cannot be taken into consideration because the prediction does not represent an external prediction as procymidone was present in the training set. We observed a low acute toxicity as this endpoint with values which varied for the several degradation products between 1000 and approximately 6000 mg/kg except for compounds 2 and 5 for which those values were estimated at 302 and 590 mg/kg, respectively, is

thus considered as moderately toxic. Compound 2, the 3,5-DCA, was reported also in the literature as of moderate acute toxicity in mice in coherence with the QSAR-predicted rat LD₅₀.^[35] Based on the overall effects on renal function and morphology, Lo *et al.*^[36] found that 3,5-DCA is the most nephrotoxic of the dichloroanilines and that it can cause acute kidney toxicity in rats which may justify the predicted LD₅₀.

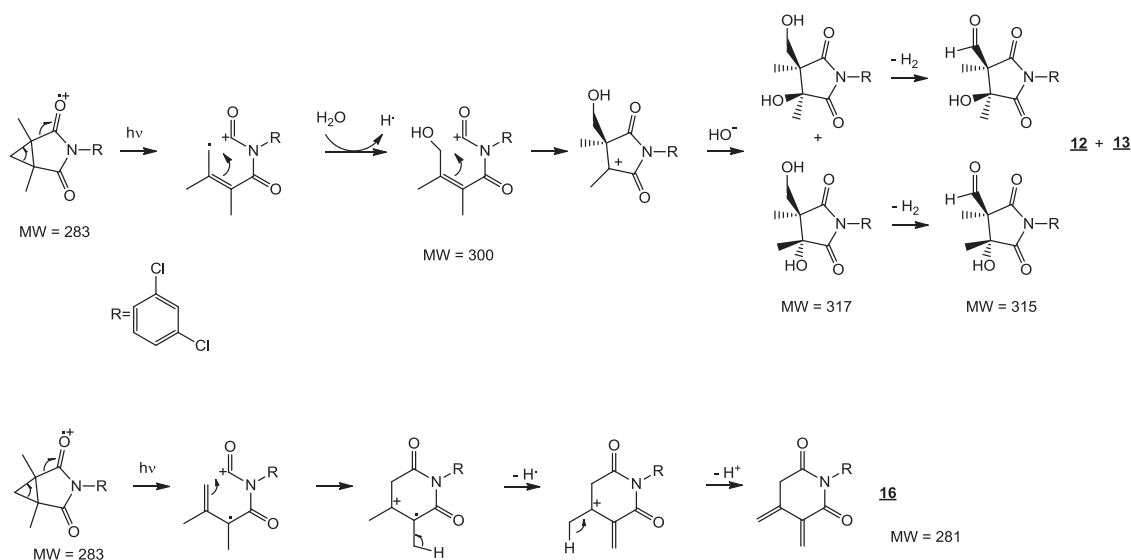


Figure 8. Mechanisms proposed to explain the formation of compounds **12**, **13** and **16** from irradiated procymidone in water.

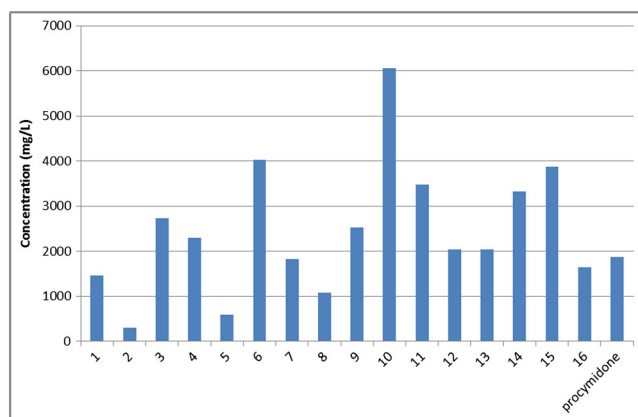


Figure 9. Oral rat LD₅₀ toxicity (mg/kg) of procymidone and photoproducts.

CONCLUSIONS

The UV-visible photodegradation of procymidone in water led to 16 photoproducts of significant abundance, three of them remaining persistent after 90 min of irradiation. Chemical structures were proposed on the basis of multi-stage collision-induced dissociation experiments. Structures were assigned also considering kinetics data and the likely evolution of irradiated species in the aqueous phase. The results on toxicity estimation showed that possible developmental toxicity could be generated through the photolytic process of procymidone; 3,5-dichloroaniline, one of the persistent products, might be responsible for this potential toxicity. An *in vitro* bioassay should then be achieved to further investigate the toxicological behavior of those degradates.

SUPPORTING INFORMATION

Additional supporting information may be found in the online version of this article.

REFERENCES

- [1] J. Martins, C. Esteves, A. Limpo-Faria, P. Barros, N. Ribeiro, T. Simoes, M. Correia, C. Delerue-Matos. Analysis of six fungicides and one acaricide in still and fortified wines using solid-phase microextraction-gas chromatography/tandem mass spectrometry. *Food Chem.* **2012**, 132, 630.
- [2] E. Pose-Juan, B. Cancho-Grande, R. Rial-Otero, J. Simal-Gandara. The dissipation rates of cyprodinil, fludioxonil, procymidone and vinclozoline during storage of grape juice. *Food Control* **2006**, 17, 1012.
- [3] European Commission. *Journal officiel de l'Union européenne*, **2010**, vol. 9.
- [4] Y. Souissi, S. Bourcier, S. Bouchonnet, C. Genty, M. Sablier. Estrone direct photolysis: By-product identification using LC-Q-TOF. *Chemosphere* **2012**, 87, 185.
- [5] G. D. Charles, H. L. Kan, M. R. Schisler, B. Bhaskar Gollapudi, M. Sue Marty. A comparison of *in vitro* and *in vivo* EDSTAC test battery results for detecting antiandrogenic activity. *Toxicol. Appl. Pharmacol.* **2005**, 202, 108.
- [6] M. B. Rosen, V. S. Wilson, J. E. Schmid, L. E. Gray. Gene expression analysis in the ventral prostate of rats exposed to vinclozolin or procymidone. *Reprod. Toxicol.* **2005**, 19, 367.
- [7] European Union. 3600/92DE. *Official Journal of the European Union* **1992**, 4.
- [8] K. Inawaka, M. Kawabe, S. Takahashi, Y. Doi, Y. Tomigahara, H. Tarui, J. Abe, S. Kawamura, T. Shirai. Maternal exposure to anti-androgenic compounds, vinclozolin, flutamide and procymidone, has no effects on spermatogenesis and DNA methylation in male rats of subsequent generations. *Toxicol. Appl. Pharmacol.* **2009**, 237, 178.
- [9] O. o. P. P. a. T. Substances. Report of the Food Quality Protection Act (FQPA) Tolerance Reassessment Progress and Risk Management Decision (TRED) for Procymidone. United States Environmental Protection Agency, **2005**.
- [10] A. Kiss, S. Rapi, C. Csutoras. GC/MS studies on revealing products and reaction mechanism of photodegradation of pesticides. *Microchem. J.* **2007**, 85, 13.
- [11] H. D. Burrows, L. M. Canle, J. A. Santaballa, S. Steenken. Reaction pathways and mechanisms of photodegradation of pesticides. *J. Photochem. Photobiol. B* **2002**, 67, 71.

- [12] K. Hustert, P. N. Moza. Photochemical degradation of dicarboximide fungicides in the presence of soil constituents. *Chemosphere* **1997**, *35*, 33.
- [13] W. Schwack, B. Bourgeois, F. Walker. Fungicides and photochemistry photodegradation of the dicarboximide fungicide procymidone. *Chemosphere* **1995**, *31*, 4033.
- [14] A. Vanni, R. Gamberini, A. Calabria, P. Nappi. Determination and identification of metabolites of the fungicides Iprodione and Procymidone in compost. *Chemosphere* **2000**, *41*, 1431.
- [15] A. G. Frenich, J. L. M. Vidal, M. M. Galera. Use of the cross-section technique linked with multivariate calibration methods to resolve complex pesticide mixtures. *Anal. Chem.* **1999**, *71*, 4844.
- [16] S. Grimme. Accurate description of van der Waals complexes by density functional theory including empirical corrections. *J. Comput. Chem.* **2004**, *25*, 1463.
- [17] S. Grimme, J. Antony, S. Ehrlich, H. Krieg. A consistent and accurate *ab initio* parametrization of density functional dispersion correction (DFT-D) for the 94 elements H-Pu. *J. Chem. Phys.* **2010**, 132.
- [18] U. o. K. a. F. K. GmbH. in TURBOMOLE GmbH, **2012**. Available: www.turbomole.com.
- [19] C. Hattig, F. Weigend. CC2 excitation energy calculations on large molecules using the resolution of the identity approximation. *J. Chem. Phys.* **2000**, *113*, 5154.
- [20] C. Clavaguera, F. Piuze, J.-P. Dognon. Electronic spectrum of tryptophan-phenylalanine. A correlated *ab initio* and time-dependent density functional theory study. *J. Phys. Chem. B* **2009**, *113*, 16443.
- [21] U. S. E. P. Agency, in Risk Management Sustainable Technology, **2012**. Available: <http://www.epa.gov/ordntrnt/ORD/NRMRL/std/qsar/qsar.html>.
- [22] L. H. Hall, B. Mohny, L. B. Kier. The electrotopological state - structure information at the atomic level for molecular graphs. *J. Chem. Inf. Comput. Sci.* **1991**, *31*, 76.
- [23] B. Gilbert-López, J. F. García-Reyes, A. R. Fernández-Alba, A. Molina-Díaz. Evaluation of two sample treatment methodologies for large-scale pesticide residue analysis in olive oil by fast liquid chromatography–electrospray mass spectrometry. *J. Chromatogr. A* **2010**, *1217*, 3736.
- [24] T. Cajka, J. Hajslova, O. Lacina, K. Mastovska, S. J. Lehotay. Rapid analysis of multiple pesticide residues in fruit-based baby food using programmed temperature vaporiser injection–low-pressure gas chromatography–high-resolution time-of-flight mass spectrometry. *J. Chromatogr. A* **2008**, *1186*, 281.
- [25] T. Alapi, K. Van Craeynest, H. Van Langenhoeve, J. Dewulf, A. Dombi. Direct VUV photolysis of chlorinated methanes and their mixtures in a nitrogen stream. *Chemosphere* **2007**, *66*, 139.
- [26] T. Alapi, A. Dombi. Direct VUV photolysis of chlorinated methanes and their mixtures in an oxygen stream using an ozone producing low-pressure mercury vapour lamp. *Chemosphere* **2007**, *67*, 693.
- [27] S. Coffinet, A. Rifai, C. Genty, Y. Souissi, S. Bourcier, M. Sablier, S. Bouchonnet. Characterization of the photodegradation products of metolachlor: structural elucidation, potential toxicity and persistence. *J. Mass Spectrom.* **2012**, *47*, 1582.
- [28] NIST/EPA/NIH. *NIST Mass Spectral Library*. National Institute of Standard and Technology, Washington DC, **2005**.
- [29] F. W. McLafferty. *Interpretation of Mass Spectra*, (3rd edn.), University Science Books, Mill Valley, CA, **1980**.
- [30] J. Ostby, W. Kelce, C. Lambright, C. Wolf, P. Mann, J. L. Gray. The fungicide procymidone alters sexual differentiation in the male rat by acting as an androgen-receptor antagonist in vivo and in vitro. *Toxicol. Ind. Health* **1999**, *15*, 80.
- [31] M. F. Cengiz, M. Certel, B. Karakaş, H. Göçmen. Residue contents of captan and procymidone applied on tomatoes grown in greenhouses and their reduction by duration of a pre-harvest interval and post-harvest culinary applications. *Food Chem.* **2007**, *100*, 1611.
- [32] P. R. Jacobsen, M. Axelstad, J. Boberg, L. K. Isling, S. Christiansen, K. R. Mandrup, L. O. Berthelsen, A. M. Vinggaard, U. Hass. Persistent developmental toxicity in rat offspring after low dose exposure to a mixture of endocrine disrupting pesticides. *Reprod. Toxicol.* **2012**, *34*, 237.
- [33] USEPA. Reregistration Eligibility Decision (RED) Iprodione. Prevention, Pesticides and Toxic Substances. EPA738-R -98-019, **1998**.
- [34] J. B. Lee, H. Y. Sohn, K. S. Shin, J. S. Kim, M. S. Jo, C. P. Jeon, J. O. Jang, J. E. Kim, G. S. Kwon. Microbial biodegradation and toxicity of vinclozolin and its toxic metabolite 3,5-dichloroaniline. *J. Microbiol. Biotechnol.* **2008**, *18*, 343.
- [35] *Pesticide Residues in Food 2007: Joint FAO-WHO Meeting on Pesticide Residues*. WHO, Food and Agriculture Organization of the United Nations, **2007**.
- [36] H.-H. Lo, P. I. Brown, G. O. Rankin. Acute nephrotoxicity induced by isomeric dichloroanilines in Fischer 344 rats. *Toxicology* **1990**, *63*, 215.